

The Evolution of the Dark Halo Spin Parameters λ and λ' in a Λ CDM Universe: The Role of Minor and Major Mergers

Helmut Hetznecker^{1*}, Andreas Burkert^{2†}

¹Max-Planck-Institut für Astronomie, Königstuhl 17, D-69117 Heidelberg, Germany,

²University Observatory Munich, Scheinerstr. 1, D-81679, München, Germany

Submitted to MNRAS

ABSTRACT

The evolution of the spin parameter of dark halos and the dependence on the halo merging history in a set of dissipationless cosmological Λ CDM simulations is investigated. Special focus is placed on the differences of the two commonly used versions of the spin parameter, namely $\lambda = JE^{1/2}G^{-1}M^{-5/2}$ (Peebles 1980) and $\lambda' = J/[\sqrt{2}M_{\text{vir}}R_{\text{vir}}V_{\text{vir}}]$ (Bullock et al. 2001). Though the distribution of the spin transfer rate $T_{\lambda}^{(\prime)} := \lambda_{\text{fin}}^{(\prime)}/\lambda_{\text{init}}^{(\prime)}$ (which is the ratio of spin parameters after and prior to merger) is similar to a high degree for both λ and λ' , we find considerable differences in the time evolution: while λ' is roughly independent of redshift, λ turns out to increase significantly with decreasing redshift. This distinct behaviour arises from small differences in the spin transfer distribution of accreted material. The evolution of the spin parameter is strongly coupled with the virial ratio $\eta := 2E_{\text{kin}}/|E_{\text{pot}}|$ of dark halos. Major mergers disturb halos and increase both their virial ratio η and spin parameter $\lambda^{(\prime)}$ for 1 – 2 Gyrs. At high redshifts $z = 2 - 3$ many halos are disturbed with an average virial ratio of $\bar{\eta} \approx 1.3$ which approaches unity until $z = 0$. We find that the redshift evolution of the spin parameters is dominated by the huge number of minor mergers rather than the rare major merger events.

Key words: cosmology: dark matter halos, angular momentum, spin parameter, mergers – methods: numerical

1 INTRODUCTION

It is among the puzzling tasks within the theory of galaxy formation to understand the origin and history of angular momentum both of dark matter halos and embedded galactic disks. One reason for the high relevance of galactic spin is that it determines the most basic properties of a galactic disc, its surface density distribution and its spatial extension through the equilibrium of gravitational and centrifugal forces, as discussed already by Hoyle as early as 1949 (Hoyle 1949). A kind of basic picture of galactic evolution has emerged in the undertow of the seminal works of White & Rees (1978) and Fall & Efstathiou (1980), which connects the angular momentum of a dark halo to its mass growth history (see also Blumenthal et al. 1986, Mo, Mao & White 1998, van den Bosch 2000, Cole et al. 2000, Somerville, Primack & Faber 2001, Kauffmann, White & Guiderdoni 1993).

Until the beginning of this century it was considered as established that bound cosmological structures gain most of their angular momentum by the tidal effect of the large scale mass distribution: After a merger the remnant is left with the angular momentum imprint of the tidal field. In recent years it was realized that yet another effect is contributing to a halo’s angular momentum history to at least the same degree as large scale tidal forces, namely its discrete mass acquisition history (Gardner 2001, Vitvitska et al. 2001, Maller, Dekel & Somerville 2002). In this scenario, orbital angular momentum is transferred to the remnant’s internal angular momentum during a merger. Statistically, the net angular momentum of a large number of mergers would be zero (if infall occurs from random directions). However, due to the low number of major mergers that occur during a halo lifetime, randomization is ineffective and there remains an imprint on the halo’s spin parameter by the final (and often only) major merger. Mergers of dark matter halos and galaxies thus moved to the center of interest not only in the field of early type galaxy formation but also in the context of

* E-mail: hetzneck@mpia.de

† E-mail: burkert@usm.uni-muenchen.de

angular momentum acquisition (Burkert & D’Onghia 2004. D’Onghia & Burkert 2004).

The angular momentum of dark matter halos is usually parametrised in terms of a dimensionless quantity, the spin parameter λ . This parameter appears in two versions; the first, original one was introduced by Peebles (1980). A revised formula was later proposed by Bullock et al. (2001) in order to overcome the energy dependence of the classic version.

In no study so far the differences between the classical λ and the revised version λ' have been investigated in detail. This is the main ambition of our work. For this purpose we analyse the data of 82 dissipationless numerical simulations of dark matter halo formation in a comoving cube of 20 Mpc starting with redshift $z=2.8$. In order to understand our results we also investigate the connection between the spin parameters and the time dependent virial coefficient $\eta = 2E_{\text{kin}}/|E_{\text{pot}}|$.

In §2 we describe the numerical simulations in detail. §3 analyses of the merger anatomy and statistics. A detailed investigation of the spin transfer in merger and accretion events is given in §4 and §5, with special attention drawn to the differences between the two λ -versions. In §6 we investigate the virial parameter of dark halos and its connection with the spin parameters. The global time evolution of λ and λ' is shown in §7. Finally we summarize and discuss our results in §8.

2 NUMERICAL SIMULATIONS

We employ the *GRAFIC* code which is part of the *COSMICS* package developed by E. Bertschinger (Ma & Bertschinger 1995) to set up random Gaussian initial conditions. In total, 82 dissipationless cosmological Λ CDM simulations are performed with different random seeds for the initial fluctuation field, using a N-Body code with a Barnes-Hut tree method (Barnes & Hut 1986) in combination with the special purpose hardware *GRAPE-3* (Makino & Funato 1993, Ebisuzaki et al. 1993). Each run represents a 20Mpc comoving cube with the standard cosmological parameters $\Omega_m = 0.7$, $\Omega_\Lambda = 0.3$, $h = 65$ and $\sigma_8 = 1.13$ ¹. The simulations start at redshifts $40 < z_{\text{init}} < 53$ (depending on when the maximum overdensity reaches unity) and follow the nonlinear evolution of 64^3 particles until $z = 0$. Position and velocity data are stored at 21 different redshifts marking approximately equal time intervals. The gravitational potential is smoothed within 7.8 comoving kpc around individual particles, each of which represents $1.07 \times 10^9 M_\odot$ of cold dark matter.

We identify halos using the friends-of-friends (FOF, see e.g. Götz, Huchra & Brandenberger 1998) algorithm with a linking length parameter of 0.2 in units of mean particle distance. Each FOF cluster of particles is truncated at a

radius R_{vir} which defines a sphere around the most bound particle within which the mean density is $\Delta(z)\rho_c(z)$, $\rho_c(z)$ being the critical density at redshift z . Following the spherical collapse model, $\Delta(z)$ would be constant in an Einstein-de Sitter universe, with $\Delta = 18\pi^2 \approx 178$ (see e.g. Peebles 1980). Due to the model dependence of the density parameter $\Omega(z) = (\Omega_m - 1)^3 \Gamma(z; \Omega_m, \Omega_\Lambda)$ this does not hold for a low density model like the one considered here. Neglecting radiative contribution to the mean cosmological density, $\Delta(z)$ takes the general form

$$\Delta(z) = 18\pi^2 + 82f(z) - 39f(z)^2, \quad (1)$$

where

$$f(z) = \frac{\Omega_m(1+z)^3}{\Omega_m(1+z)^3 + \Omega_\Lambda} - 1 \quad (2)$$

(Bryan & Norman 1998).

Our simulations yield a total number of 10563 halos, each with more than 100 particles at $z = 0$. In order to avoid a mass truncation bias in our merger trees, we consider only halos which contain at least 500 particles at present epoch, corresponding to a minimum halo mass of $5.35 \times 10^{11} M_\odot$ which leads to a sample of 2383 halos; particle clusters as small as 50 particles ($1.07 \times 10^{11} M_\odot$) are nevertheless taken into account as progenitors and satellites at higher redshifts. Note that throughout this study we didn’t detect any mass dependence of our results, which therefore should be valid for lower mass halos as well.

We construct merger trees for the complete sample of halos with $M(z=0) > 5.35 \times 10^{11} M_\odot$ in the following way: A major merger (MM) is defined to be an event where two initially separated halos appear FOF-bound in the next data output with 3 restrictions:

- the less massive, infalling clump (denoted as the *satellite*) has a fraction of at least $m_h \geq 1/5$ of the larger clump’s (the *halo*’s) mass.
- the merger remnant contains more than 60% of the initial satellite’s particle reservoir
- the massive progenitor halo has a mass of at least 40% of its mass at $z = 0$.

The first restriction separates mergers from events which we will denote as ”accretion” or ”minor mergers” (mM) throughout. Note that we do not distinguish between minor mergers and accretion; both terms correspond to any detected matter acquisition which increases the progenitor’s mass by less than 20%. The second criterion guarantees that the mass growth after the preceding time step does in fact originate from the satellite infall and not from accretion or mM events which may well happen during the same time period. The third point finally rules out mergers which, due to the low mass of the remnants, do not have a significant impact on the dynamics of the final halo or galaxy at $z = 0$. It is clear that our particular choice of the parameter values (60% and 40% in the 2nd and 3rd item, respectively) is somewhat arbitrary and lacks a quantitative justification. Nevertheless it seems plausible that this choice of numbers is suitable for the purposes described above. By identifying all progenitor-remnant relations throughout all data outputs we construct a list of progenitors of each halo at $z = 0$ as well as the according mass acquisition history.

¹ Note that these simulations were performed earlier than the current WMAP results ($\sigma_8 = 0.9 \pm 0.1$, see Spergel et al. 2003) were published. Our value for σ_8 is following the expression $\sigma_8 = (0.5 \dots 0.6)\Omega^{-0.56}$ from White, Efstathiou & Frenk (1993). We don’t expect this discrepancy to affect our results. Especially results concerning individual merger events should be completely unaffected.

3 MERGER STATISTICS AND ORBITAL PARAMETER

Before we are going to examine the spin evolution of dark matter halos in detail we want to "set the stage" by briefly discussing the abundance and the orbital characteristics of major mergers.

3.1 Orbital Parameters

Certainly the main quantity that characterizes the dynamics of a major merger is the mass ratio of the involved halos. The dynamical properties of the remnant, however, depend on both the internal and orbital energy and angular momentum contributions. If we describe the approach of two halos following the Kepler laws for classical two body systems (which is well justified as long as the objects are spatially separated), the orbital energy and angular momentum content of the system is fully described by their orbital parameters. The *eccentricity* is usually defined by

$$\epsilon = \left[1 + \frac{2EL^2}{\mu(Gm_h m_s)^2} \right]^{1/2}, \quad (3)$$

where E and L are the total orbital energy and angular momentum, μ is the reduced mass, G the gravitational constant and m_h and m_s are the masses of the halo and the satellite, respectively. The second parameter, the *pericenter distance* corresponds to the fictitious closest approach of the objects (pretending the system would continue to behave like a perfect two body system long enough) and is given by

$$R_{\text{peri}} = \frac{L^2}{\mu G m_h m_s (1 + \epsilon)}. \quad (4)$$

We find that 90% of all mergers have bound orbits ($\epsilon < 1$) and 71% have values of $0.9 < \epsilon < 1$. This clear maximum of $p(\epsilon)$ close to unity can be considered as the main feature of the eccentricity distribution. Note that initially unbound hyperbolic orbits are as well compatible with merger events since orbital energy can be transformed to internal one during the merger.

For the pericenter distance R_{peri} we find a probability distribution which can be well described by $P(R_{\text{peri}}/R_{\text{vir}}) = A \exp(-\alpha \times R_{\text{peri}}/R_{\text{vir}})$, where $(A, \alpha) \approx (0.089, 5.0)$ for $R_{\text{peri}}/R_{\text{vir}} > 0.2$ and $(0.12, 6.3)$ for $R_{\text{peri}}/R_{\text{vir}} < 0.2$. The mean relative pericenter distance turns out to be $0.18R_{\text{vir}}$.

We finally checked the distribution of the angles β between the spin planes of halos and infalling satellites. In agreement with expectations we find a distribution that is well fitted by $dN/d\beta \propto \sin \beta$.

Khochfar & Burkert (2003, KB2003) investigated in very detail the statistics of various merger orbital parameters using a huge data sample provided by the VIRGO consortium. Apart from minor deviations we find the results from this section to be in good agreement with KB2003.

3.2 Merger Statistics

The internal structure of dark matter halos and their embedded galaxies is to a high degree sensitive to their merging histories. Strong evidence exists now that elliptical galaxies originate from MM events (see Toomre & Toomre 1972, Naab, Burkert & Hernquist 1999, see Burkert & Naab 2003,

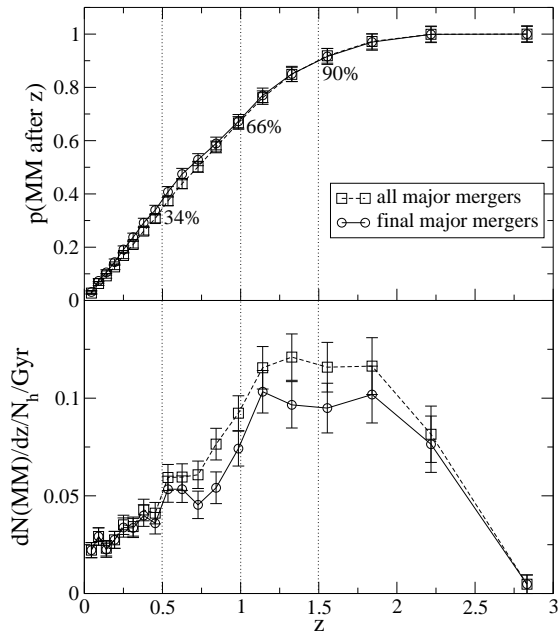


Figure 1. Top panel: cumulative redshift distribution of major mergers. The vertical axis shows the fraction of mergers later than redshift z in our simulations. Lower panel: Merger rate at redshift z , i.e. the number of mergers per unit time normalized to the total number of halos with masses above $5.35 \times 10^{11} M_{\odot}$.

2004 for a reviews). As will be discussed in this paper, the evolution of a dark halo's spin parameter seems as well to be a matter of the mass growth history (see also D'Onghia & Burkert 2004). Therefore it is worth to illustrate the mean merger history of our sample of dark halos throughout their evolution. The top panel of Fig.1 shows the probability for a dark halo to have a (final) MM at redshift smaller than z (if it has a MM at all), while the lower one shows the number of (final) MMs per time, normalized to the total number of halos with masses higher than $m_{\text{min}} > 5.35 \times 10^{11} M_{\odot}$ (corresponding to 500 particles minimum). The so defined merging rate shows a broad maximum between redshift 1.2 and 1.8, where the rate is roughly constant. After $z \approx 1$ as well as before $z \approx 2$ the rate is continuously decreasing to a value of $\approx 0.02 \pm 0.004/N_h/\text{Gyr}$ and $0.05 \pm 0.005/N_h/\text{Gyr}$ at $z = 0$ and $z = 2.8$, respectively, where N_h is the total number of halos above m_{min} at the corresponding redshift. Roughly one third of all MMs occur in redshift intervals of $z = 0 - 0.5$, $0.5 - 1$ and $1 - \infty$ (see top panel of Fig.1). This shows that the spin parameter of dark halos may undergo changes throughout its whole lifetime, if the spin is affected by these merger events.

4 SPIN TRANSFER IN ACCRETION AND MERGER EVENTS

In the commonly established scenario, cosmic structures acquire angular momentum by tidal interaction with the sur-

rounding matter distribution (Barnes & Efstathiou 1987, Padmanabhan 1993 and first Hoyle 1949). This mechanism works most effectively during the early expansion and collapse phase, when the large spatial extension of the protohalo offers a large lever for tidal forces. The Zel'dovich approximation is a powerful tool for an analytical treatment of the spin acquirement and it turns out that angular momentum is growing linearly with time until the point of turnaround is reached.

More recently, cosmologists became aware of merger events to have a significant impact on the halos' spin by the transfer of orbital to internal angular momentum (Gardner 2001, Vitvitska et al. 2001 (VK01)). It appears plausible that the quantitative evolution of spin transfer in mergers is depending on the corresponding orbital parameters. This complicates the investigation of the spin evolution in so far as we have to deal with nonlinear physics which rules out an ab initio analytical description like the linear tidal torque theory.

4.1 Spin Transfer Statistics

To explore the merger impact on the halo spin parameter in detail, the most basic investigation is to analyse the probability of a single merger event to rise (or decrease) the spin of a halo by a certain amount. The alteration of spin is quantified simply by the spin transfer

$$T_\lambda := \lambda_{\text{fin}}/\lambda_{\text{init}}, \quad (5)$$

where λ_{fin} is the (final) spin parameter of the merger remnant and the initial λ_{init} corresponds to its main progenitor. We want to highlight the characteristics and differences of both established versions of dimensionless spin parameter definitions throughout this paper. The earlier classical version introduced by Peebles (1980) reads

$$\lambda = \frac{J\sqrt{E}}{GM_{\text{vir}}^{5/2}}. \quad (6)$$

Here J is the modulus of the total angular momentum, E is the absolute value of the total (kinetic plus potential) energy and M is the mass of the halo under consideration. All quantities are calculated using the set of particles within the virial radius R_{vir} . Bullock et al. (2001) later defined an alternative version, namely

$$\lambda' = \frac{J}{\sqrt{2}M_{\text{vir}}R_{\text{vir}}V_{\text{vir}}}, \quad (7)$$

where $V_{\text{vir}} = GM_{\text{vir}}R_{\text{vir}}^{-1}$ is the circular velocity at the virial radius R_{vir} . This latter (dashed) quantity is more frequently applied in practical analysis due to its independence of the density profile. Both quantities are nevertheless approximately identical for halos with NFW profiles (Navarro, Frenk & White 1996) and concentration parameter $c \approx 10$ as well as isothermal halos truncated at R_{vir} (Maller, Dekel & Somerville 2002).

Fig. 2 shows the λ -distribution for all halos at $z = 0$ and for the merger and accretion dominated subsamples of halos as well. One can clearly see a shift between each sample corresponding to the according spin transfer behaviour: As to expect, MM dominated halos are shifted to higher λ values, mM halos occupy lower values. In each case the distribution

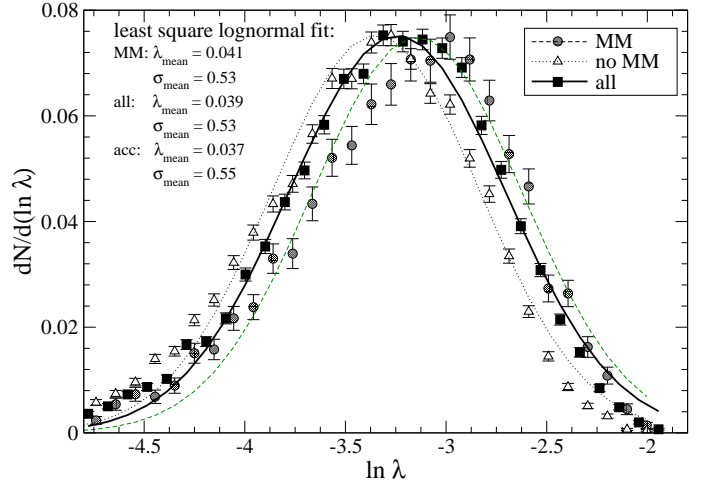


Figure 2. Distribution of the (classical) spin parameter λ . Each sample (halos with MMs, without MMs and full sample) is following roughly a lognormal distribution (see e.g. Cole & Lacey, 96). Depending on the merger history the distribution is shifted to higher (MM sample) or lower (mM sample) values.

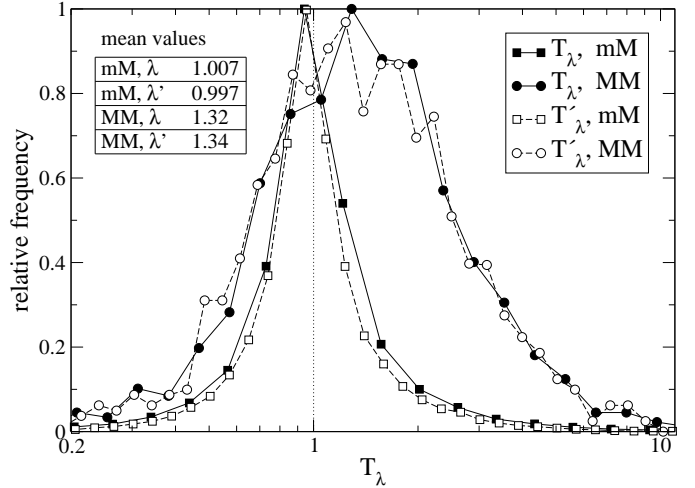


Figure 3. Distribution of the spin transfer rates $T_\lambda = \lambda_{\text{fin}}/\lambda_{\text{init}}$ (full lines) and $T'_\lambda = \lambda'_{\text{fin}}/\lambda'_{\text{init}}$ (dashed lines) for major (circles) and minor mergers (squares). Clearly major mergers provide a source of angular momentum: roughly two third of all MMs increase the spin parameter; in the case of minor mergers less than half of all events increase λ by a moderate amount. Note that the behaviours of T_λ and T'_λ are hardly distinct for either merger type. See the discussion in the text for details.

is roughly lognormal. Here we do not show the distribution of λ' but note that we find a similar behaviour.

Fig.3 shows the distribution of the spin transfer rates T_λ and $T'_\lambda := \lambda'_{\text{fin}}/\lambda'_{\text{init}}$ for the case of major ($m_s > 0.2m_h$) and minor merger/accretion ($m_s < 0.2m_h$) events. In the following discussion all numbers concerning λ' are listed in brackets behind the numbers corresponding to the undashed λ .

Fig.3 clearly shows that MMs rise the spin parameter by a significant amount: 68% (67%) of all MMs rise $\lambda^{(l)}$. In more than 50% of all MMs, $\lambda^{(l)}$ is increased by a factor of 1.30 (1.31). This is in good agreement with the previous study of VK01 who found a median of 1.25 for the dashed quantity T'_λ . For the according mean values we find $\overline{T'_\lambda^{(l)}}$ are 1.32 (1.34).

As expected the situation is different for the case of mM and accretion events. Again there are both, spin-rising and decreasing events, but now with a clear shift to a lower T_λ regime: The distribution of T_λ in this case is significantly narrower and approximately symmetric around unity, with a linear median value of $T_\lambda = 0.98(0.99)$ and a mean of 1.007 (0.997). 53% (56%) of all events decrease the spin parameter.

It turns out that the behaviour of both spin parameters is very similar in the above context, regardless of the density profile dependence of λ/λ' which should lead to visible differences especially during the merging phase, where the density distribution is strongly time dependent. Nevertheless the tiny difference of the \overline{T}_λ and $\overline{T'_\lambda}$ distribution in the accretion case has striking effects on the global time evolution of λ and λ' . We will discuss this important issue in detail in §7.

4.2 Dependence on Orbital Parameters

As mentioned before, the plausible explanation for the qualitative behavior just described is that orbital angular momentum and the spin of the satellite are transferred to internal spin of the remnant during the merging process, according to

$$\vec{J}_{\text{remn}} \approx \vec{J}_{\text{prg}} + \vec{J}_{\text{sat}} + \vec{L}_{\text{orbit}} \quad (8)$$

where the indices represent remnant, progenitor, satellite and the system's orbit respectively. Exact equality is unlikely since some dark matter particles are lost during the merging process. $T_\lambda^{(l)}$ is more or less sensitive to the relative orientation of the vectors on the right hand side of Equ. (8), depending on the relation of their absolute values. Since we are discussing major merger events it is justified to assume satellites and halos to have internal angular momenta of the same order of magnitude. From Fig.4 one can see that only in a small fraction (4%) of all MMs the halo internal angular momentum is larger than L_{orbit} . In 80% of all events $L_{\text{orbit}} > 3 \times J_{\text{prg}}$ and still for every third case $L_{\text{orbit}} > 7.7 \times J_{\text{prg}}$. This demonstrates directly that the spin transfer is dominated by the orbital angular momentum. We find a small but detectable dependence of T_λ on the vector angles $\alpha_{\vec{L}_{\text{orbit}} \vec{J}_{\text{prg}}}$ and $\alpha_{\vec{J}_{\text{prg}} \vec{J}_{\text{sat}}}$. The bottom panel of Fig.5 shows a linear fit through the median T_λ -angle plot. Though suffering from a large scatter, there is a clearly visible trend of increasing spin transfer with decreasing spin-orbit- and spin-spin-angle.

If the transfer of angular momentum is dominated by L_{orbit} we should also expect a more elementary dependence of T_λ on the pericenter distance since (for fixed eccentricity ϵ) R_{peri} is proportional to the satellites' impact parameter p_i which, for its part, satisfies $L_{\text{orbit}} \propto vp_i$. In Fig.5 (upper panel) T_λ is plotted against R_{peri}/R_{200} which is well fitted by the power law

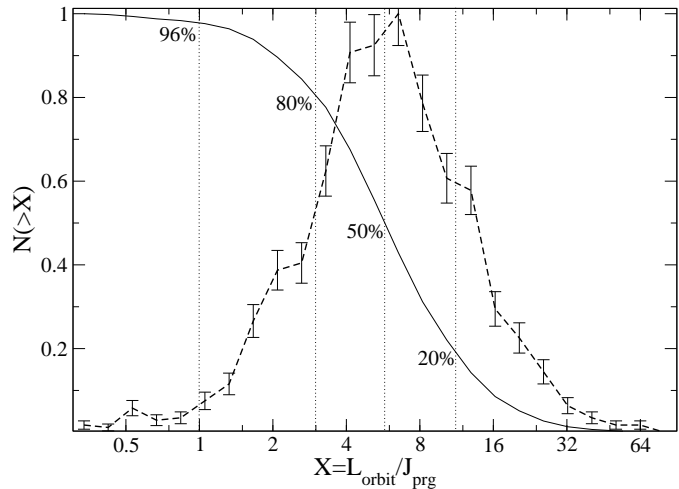


Figure 4. Cumulative (full line) and differential (dashed line) distribution of the ratios of orbital to internal angular momentum. In 50% of all mergers $L_{\text{orbit}} > 6 \times J_{\text{prg}}$. In less than 4% of all cases $J_{\text{prg}} > L_{\text{orbit}}$. The diagram demonstrates that the spin transfer is dominated by the orbital angular momentum.

$$T_\lambda \propto \left[\frac{R_{\text{peri}}}{R_{200}} \right]^{0.18} \quad (9)$$

over a R_{peri}/R_{200} range of almost 3 orders of magnitude. This clearly reflects the leading role of the impact parameter for the amount of spin transfer in a merger event. We also investigated the according behaviour of the dashed spin transfer T'_λ and didn't find any significant difference.

5 BEFORE, DURING AND AFTER MERGING — RISING AND DECLINING SPIN

Major mergers at first appear to be the main sources for rising spin parameters in the nonlinear evolution of dark halos. The upper panel of Fig.6 however offers a more complex view: it shows the evolution of the mean $\bar{\lambda}$ along the “fictitious” time axis t^* , where the latter variable represents an individual time scale for each halo with the zero point $t^* = 0$ shifted to the halo's final major merger event. In other words, the individual curve $\lambda_j(t)$ of each halo j is shifted along the (real) time axis such that its final MM happens at the same fictitious time $t^* = 0$. The average is taken within time intervals of 0.6 Gyrs.

For $t^* < 0$ the mean spin parameter is almost constant or at most slightly increasing with a rate of $d\bar{\lambda}/dt \approx (4.8 \pm 0.8) \times 10^{-4} \text{Gyr}^{-1}$. Within the first 0.6 Gyrs after the merger onset $\bar{\lambda}$ rises fast by 30%, followed by a 5 Gyrs lasting 1st phase during which the spin decreases again with a power law $\bar{\lambda}(t^*) \propto 1/(t^*)^{0.15}$, and a 2nd phase with a further decline, following a quadratic function.

The $\lambda'(t^*)$ curve looks similar. There is a significant peak after the merger onset and a modest decline later on. Note however that both spin parameters have equal mean values only at late fictitious times t^* , i.e. well after the final mergers. For times $t^* < 3 \text{Gyr}$ λ is significantly lower than

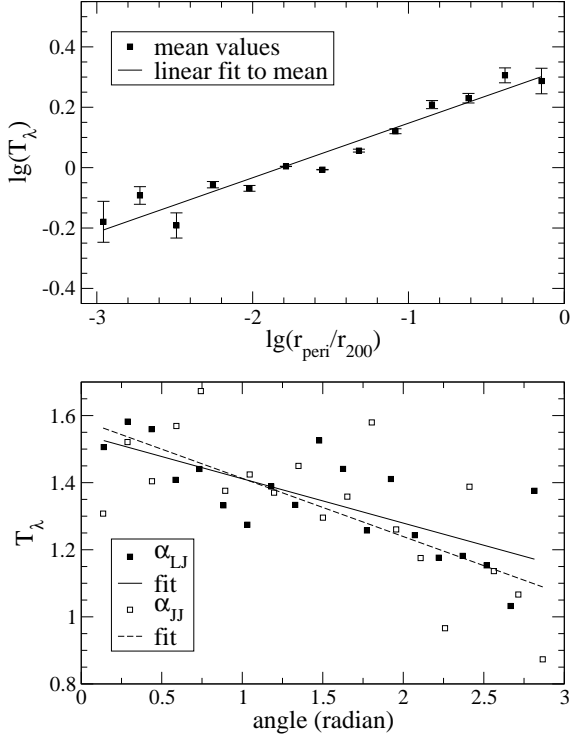


Figure 5. Top: Spin transfer T_λ vs. relative pericenter distance. The diagram shows a tight correlation following $T_\lambda \propto (R_{\text{peri}}/R_{\text{vir}})^{0.18}$. The error bars reflect the Gaussian tolerance for the mean values rather than the standard deviation of the individual merger data. Bottom: T_λ vs. spin-spin and spin-orbital angular momentum angle (α_{LJ} and α_{JJ} respectively). As typically $L_{\text{orbit}}/J_{\text{prg}} > 1$ the T_λ -angle correlation is clearly weaker than the relation between T_λ and R_{peri}

λ' , and the difference increases towards earlier times. For $t^* < 0$ λ' is also roughly constant.

To understand the behaviour of the mean spin parameters $\bar{\lambda}^{(i)}$ in further detail, it is instructive to explore the time evolution of the quantities which constitute the spin parameters, namely the angular momentum $L(t^*)$, the total energy $E(t^*)$ and the total mass $M(t^*)$ for the case of λ (Equ. (6)) and the virial radius R_{vir} and velocity V_{vir} for λ' (Equ. (7)). The results are shown in the middle and lower panel of Fig.6. Each curve is normalized to unity at the merger onset $t^* = 0$.

We consider the middle panel of Fig.6 first, representing the undashed mean $\bar{\lambda}$. Already for $t^* < 0$ the permanent smooth matter infall causes a steady growth of the total energy absolute value $|E|$, angular momentum L and mass M within the redshift dependent virial radius. Until the merger's onset the spin rising effect of \sqrt{E} and L compensates and somewhat exceeds the decreasing effect of the $M^{-5/2}$ term in the denominator of Equ.6. While the values of L and \sqrt{E} rise by factors of approximately 5 (neglecting the initial rise which is likely due to the poor statistics for $t^* < -8$ Gyrs) and 2 respectively, $M^{-5/2}$ drops by a factor of ≈ 7 during the same period.

At $t^* = 0$, a large satellite enters the halo and the mean

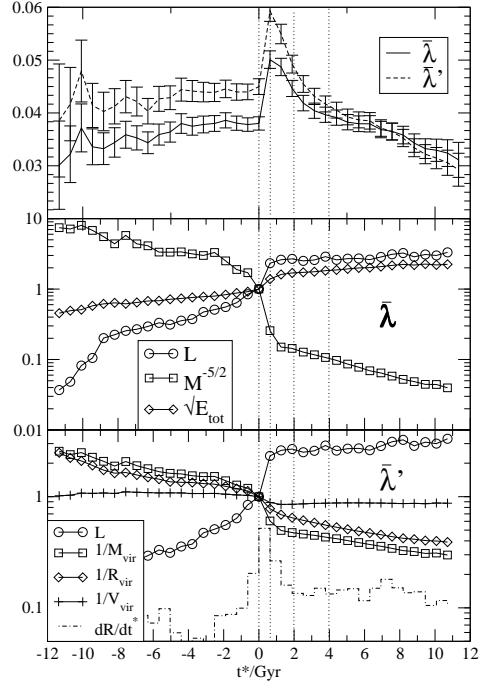


Figure 6. Top panel: Evolution of the mean spin parameters $\bar{\lambda}$ and $\bar{\lambda}'$. The time axis t^* denotes the time for each individual halo relative to its final major merger event at $t^* = 0$. The sudden rise of $\bar{\lambda}^{(i)}$ right after the merger onset is followed by a less rapid decline. The middle and bottom panel show the (relative) time evolution of the quantities that make up the spin parameters (see Eqs. (6) and (7)). In both cases, the sudden rise of the angular momentum (open circles) is responsible for the fast increase of the spin parameter after $t^* = 0$. Note also the dotted-dashed line in the bottom panel, which illustrates the differential growth of the virial radius. See text for further discussion.

angular momentum and the total energy rise by factors of 2.3 and 1.4 respectively within only 0.6 Gyrs, while the total mass term ($M^{-5/2}$) is decreasing by a factor of ≈ 0.25 . One must be careful not to simply multiply these quantities in order to predict the behaviour of $\bar{\lambda}$. Note that we are considering mean values ($\bar{L}, \bar{M}^{-5/2}, \bar{E}^{1/2}$) here, i.e. the sums of single values, while the mean spin parameter $\bar{\lambda}(t^*)$ in Fig.6 is a sum of the products of individual $\sqrt{E_j}, L_j$ and $M_j^{-2.5}$ values. Both quantities, $\bar{\lambda}(t^*)$ and $\bar{L}(t) \times \bar{E}^{1/2}(t^*) \times \bar{M}^{-2.5}(t^*)$ would be comparable only for small variances of the single values.

We can nevertheless draw some qualitative conclusions on the roles of L, E and M for the evolution of the spin parameter $\bar{\lambda}(t^*)$. Obviously, the rise of angular momentum is the quantity mainly responsible for the sudden rise of $\bar{\lambda}$ after $t^* = 0$ while the total energy seems to contribute to a minor degree. After $t^* \approx 0.6$ Gyr, when $\bar{\lambda}$ is decreasing, the figure shows that this is due to the change of the mean mass, which is continuing to increase by a factor of ≈ 5 due to accretion between the final merger and $z = 0$ while \bar{L} and $\bar{E}^{1/2}$ are not changing significantly during the same period.

The lower panel of Fig.(6) shows the situation for the case of λ' : Before $t^* = 0$ the increasing mean mass and virial

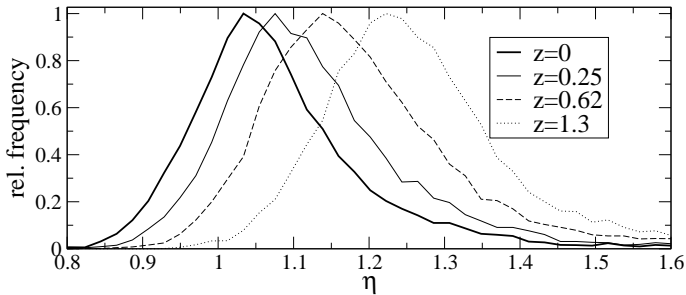


Figure 7. Distribution of the virial coefficient η at various redshifts. Note that even at $z = 0$, the distribution doesn't peak at $\eta = 1$, but is shifted to slightly higher values due to infalling material.

radius is almost canceling the effect of the increasing angular momentum. At $t^* = 0$ the spin parameter is rising by more than 30% within 0.6 Gyrs, caused by the fast rising angular momentum as in the (undashed) λ case. Later on, i.e. after $t^* = 0.6$ Gyr the growing mass and radius in combination with an almost constant mean virial velocity and angular momentum of the halo sample is responsible for $\bar{\lambda}$ to decrease.

6 THE VIRIAL COEFFICIENT η

We store our simulation data at 21 particular times between $z \approx 2.5$ and $z = 0$ with approximately equal time intervals $\Delta t \approx 6.3 \times 10^8$ yrs. We therefore can detect a MM in a phase within a period Δt after the individual virial radii of both merger partners had first contact. In such an early stage of merging the merger remnant is very disturbed and far from dynamical equilibrium. This might cause the temporary peak of the spin parameter values at $t^* \approx 0$. To investigate this question and quantify the relaxation of a halo we employ the virial parameter

$$\eta := \frac{2E_{\text{kin}}}{|E_{\text{pot}}|} \quad (10)$$

where E_{kin} and E_{pot} are the total kinetic and potential energies of all particles within R_{vir} . According to the virial theorem η should approach unity for an isolated relaxed object. Note that infalling material is affecting the surface pressure $S_p = -\int p \hat{r} \cdot d\vec{S}$ of dark halos in cosmological simulations (p is the pressure with radial direction \hat{r} on the surface element $d\vec{S}$). Since the scalar virial theorem in absence of magnetic fields reads $2E_{\text{kin}} + E_{\text{pot}} + S_p = 0$, a momentum flux induced negative surface pressure causes $2E_{\text{kin}}/|E_{\text{pot}}| > 1$ (Shapiro et al. 2004), which we indeed find for the mean virial coefficient $\bar{\eta}$ at any redshift (Fig. 8). Figure 7 shows the distribution of η and its dependence on redshift. Only a small fraction of halos have $\eta = 1$. In addition, η on average increases with increasing z while the width of the distribution remains roughly constant.

6.1 Global Time Evolution

Before we are going to consider the correlation between the spin parameters and the virial coefficient, we want to examine the time and redshift evolution of η . As shown in the top panel of Fig.8 the mean virial coefficient is clearly decreasing with decreasing redshift, well described by the quadratic function $\bar{\eta}(z) = -3.3 \times 10^{-2}(z + 2.7)^2 + 1.3$; this corresponds in good approximation to a linear decline of $\bar{\eta}$ with time, namely $\bar{\eta}(t) \approx 1.35 - 1.7 \times 10^{-2}t/\text{Gyr}$. It reflects the general tendency of halos to approach a more dynamically relaxed state, corresponding to $\eta \approx 1$, according to the fact that interactions between halos in later times are less frequent and disturb halos less than at high z .

In addition, the surface term S_p becomes less important. The lower panel of Fig.8 shows the evolution of $\bar{\eta}$ with fictitious time t^* relative to the final merger (analogous to the spin parameter evolution in §5). We find again the peak-like feature at $t^* = 0$, similar to $\lambda^{(l)}(t^*)$. At the epoch of the major merger happens, the general decline stops and $\bar{\eta}$ increases temporarily instead. Compared to the merger induced rise of $\lambda(t^*)$, the change in $\bar{\eta}$ is measurable already before the merger onset: More than 2 Gyrs before $t^* = 0$, $\bar{\eta}(t^*)$ starts to deviate significantly from the linear decline which is shown by the dashed curve in Fig. 8 and already 0.6 Gyrs before merging $\bar{\eta}$ experiences its fastest rise. Obviously the internal dynamical equilibrium of the halo is already disturbed by the proximity of a satellite; other than in the spin parameter case, the effect on η is preceding the physical contact. $\bar{\eta}$ reaches its maximum value at the same time as λ . About 2.5 Gyrs after the merger, $\bar{\eta}$ is continuing to evolve as if nothing happened, i.e. $\bar{\eta}(t^*)$ is following the same linear behaviour as before (see Fig.8). Obviously the temporary fast increase in the spin parameters shortly after a major merger is at least partly caused by the fact that the halos are out of virial equilibrium and the spin parameters achieve again a more typical value after a relaxation time which corresponds to a few dynamical timescales.

6.2 Correlation between η and $\lambda^{(l)}$

Peebles' classical definition of the spin parameter (Equ.6) makes use of both the kinetic and potential energy. Therefore one can expect a direct correlation between λ and $\eta = 2E_{\text{kin}}/|E_{\text{pot}}|$, disturbed only by the scatter of the independent angular momentum J in the definition of the spin parameter. The Bullock et al. alternative λ' is not using mechanical energies explicitly. It should nevertheless depend on relaxation since the virial radius which defines the region inside which λ is determined, is not well defined in a disturbed, unrelaxed halo.

Fig.9 shows the correlation between $\lambda^{(l)}$ and the virial coefficient η . Both λ and λ' are increasing for higher values of η , following

$$\lambda^{(l)} \approx \alpha + \beta\eta^4$$

within a range of $0.9 < \eta < 1.5$, which contains more than 90% of all halos. Two clear trends are visible:

- (i) The Bullock spin parameter λ' is significantly stronger correlated with the virial coefficient η .

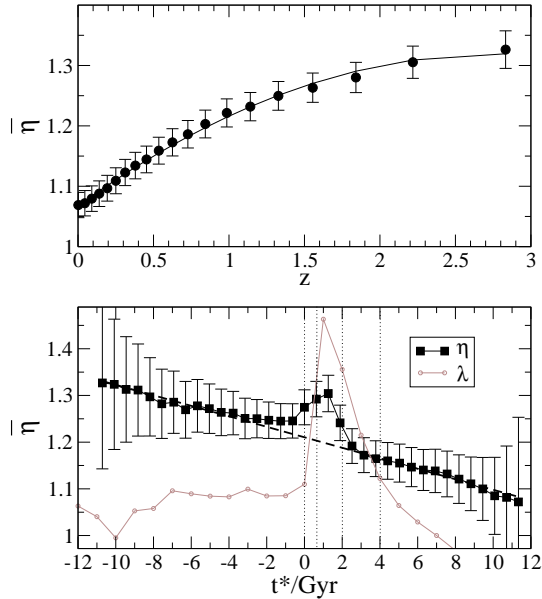


Figure 8. Top panel: Redshift evolution of the mean virial coefficient. $\bar{\eta}$ is decreasing with declining redshift, reflecting the tendency of halos to become more relaxed and infall to be less important. The quadratic decline with decreasing redshift corresponds approximately to a linear decline with time. Lower panel: The linear behaviour of $\bar{\eta}$ with vicitious time t^* is disturbed only by the merger event, analogous to the behaviour of the spin parameter (grey line). Before and after the merger $\bar{\eta}(t^*)$ is described by the same linear function (dashed line, see text for details).

(ii) The correlation becomes slightly weaker at higher redshifts.

The values of the parameters α and β can be found in the caption of Fig.9.

We finally examine the ratio of the spin parameters λ'/λ in order to further illuminate the differences in their behaviours. Fig.10 shows that λ'/λ is decreasing with time – in quite a similar manner as the virial coefficient – again featuring a hump in the vicinity of $t^* = 0$. The strong correlation between λ'/λ and η is illustrated by the $\eta/(\lambda'/\lambda)$ plot in the same figure: the linear behaviour of this quantity is only disturbed for a relatively short period directly after the merger onset, indicating that λ'/λ is falling back to a linear evolution more quickly than the virial coefficient. Note that $\eta/(\lambda'/\lambda)$ in Fig. 10 is not yet affected at $t^* = 0$ when the individual quantities already reach values close to their maximum ones. Thus the ratio λ'/λ is stronger correlated with the virial coefficient η than each spin parameter separately. This result turns out to be important for the next chapter.

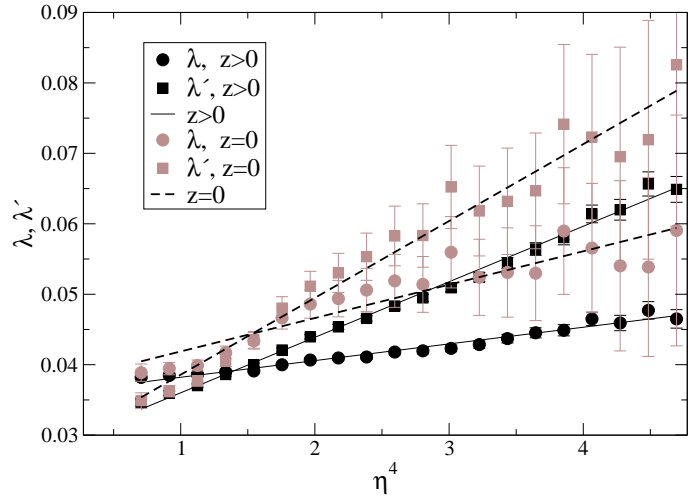


Figure 9. Spin parameter dependence of the virial coefficient η . Each case can be well fitted by $\lambda^{(i)} = \alpha + \beta \times 10^{-3} \eta^4$. The fit parameter values are $(\alpha, \beta) = (0.036, 2.4)$ for $\lambda; z > 0$, $(0.028, 7.9)$ for $\lambda'; z > 0$, $(0.037, 4.7)$ for $\lambda; z = 0$ and $(0.028, 11)$ for $\lambda'; z = 0$. $\lambda^{(i)}(\eta = 0)$ is almost independent of the redshift. Note that “ $z > 0$ ” refers to the complete sample of halos excluding only those at $z = 0$. Due to the good number statistics, the error bars of the

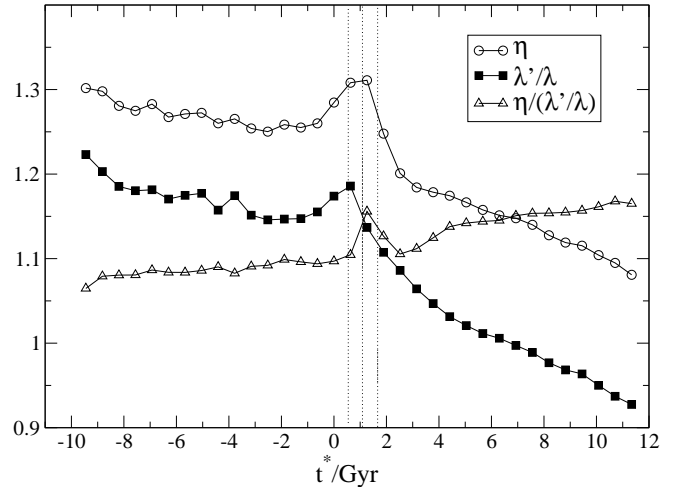


Figure 10. Evolution of the spin parameter ratio λ'/λ (full squares) with respect to the final merger event ($t^* = 0$). Plotted are also the virial coefficient η (open circles) and the ratio $\eta/(\lambda'/\lambda)$ to illustrate the strong correlation between η and λ'/λ , which is only disturbed for a short time period after the major merger.

7 TIME EVOLUTION OF THE SPIN PARAMETERS

In this chapter we want to address the question, how the sum of merging and accretion affects the global evolution of the spin parameters with cosmological time. It turned out in this work and previous ones (e.g. Vitvitska et al. 2001), that

individual MM and mM events can either rise or decrease the spin parameter: While mM events give $T_\lambda \approx 0$ on average, it is obvious that MMs tend to clearly rise λ .

The spin history of any single halo is highly chaotic as soon as the smooth phase of spin-up increase by tidal torques is left behind and non linear matter acquisition comes into play (Peirani, Mohayaee & de Freitas Pacheco 2003, Primack 2004). But if we instead consider the mean value of all halos we may still expect a smooth redshift evolution of the mean spin parameter due to the cumulative increase of the total number of mergers during the cosmic evolution shown in Fig.1.

We find this to be valid for both spin parameters with a nevertheless important and surprising difference. In Fig.11 we see that $\bar{\lambda}'$, averaged over *all* halos is approximately constant between $z = 0$ and $z \approx 2$. The mean value of the undashed classical λ in contrast is significantly increasing with cosmological time, following approximately the linear relation

$$\bar{\lambda}(z) = 0.039 - 3.5 \times 10^{-3}z. \quad (11)$$

It is instructive to consider just the mM/accretion dominated subsample of halos. First we note that the values of both λ and λ' lie well below the full sample of (MM+mM) mean values as a result of the missing angular momentum “kicks” by major mergers. But while $\bar{\lambda}'$ due to mM events decreases significantly with decreasing redshift, we find that the opposite is true for the undashed classical λ . This unveils the crucial difference between both spin parameters.

To understand this feature we consider again Fig.3 which shows the spin transfer distributions. As already mentioned, one would hardly speak of distinct behaviours between the transfer rates at first glance: We noted values of $\bar{T}_\lambda = 1.007$ and $\bar{T}'_\lambda = 0.997$ for the mM halos. In our simulation every halo suffers this rise (or reduction) of its spin parameter around 18-19 times² on average between $z = 2$ and $z = 0$. The net effect of all individual mM events is thus $\Delta\lambda^{(i)} := \lambda_{z=0}^{(i)}/\lambda_{z=2}^{(i)} = [T'_\lambda]^{19}$. For the dashed version this gives $\Delta\lambda' = 0.997^{19} \approx 0.94$, while for the classic version we get $\Delta\lambda = 1.007^{19} \approx 1.14$. Fig.11 shows that these numbers correspond roughly to the redshift evolution of either minor merger sample! Thus the tiny differences between the T_λ and T'_λ distributions lead to a distinct time evolution of the spin parameters. It is beyond the scope of this paper to analyse the detailed physical mechanisms for this difference.

According to the Fig.11, major mergers in either case have only corrective character: Though individual MMs rise the spin parameter by 130% on average, they occur too rarely to overtrump the net effect of accretion and minor mergers which act quasi permanently. We conclude that minor merger events and accretion rather than major mergers provide the driving force guiding the behaviour of the spin parameters. Their very distinct time evolution is entirely caused by tiny differences of the spin parameters’ response to accretion, while major mergers yield a minor additional

² Remember that we defined minor mergers/accretion events as any mass acquisition between two data outputs that can not be classified as major merger. The latter happens about once during a typical halo life. Since we have 20 output dumps since $z = 2$, in 19 of them we have to deal with mM events by definition

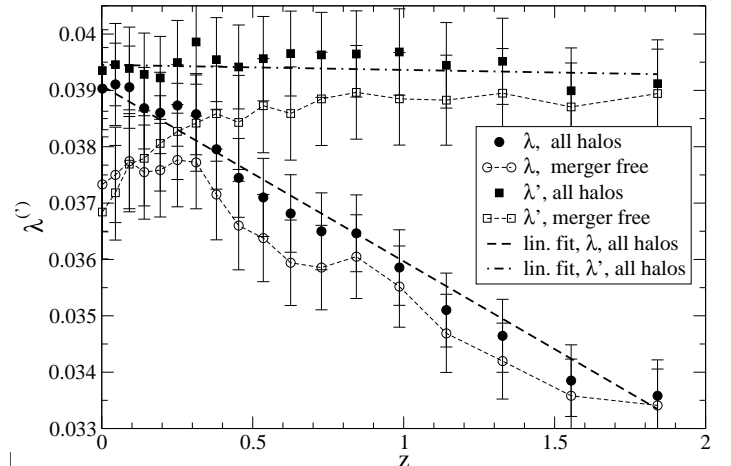


Figure 11. Redshift evolution of the mean spin parameters $\bar{\lambda}$ and $\bar{\lambda}'$ for the mM- and the full sample of halos. While $\bar{\lambda}$ is increasing with time for both halo samples, we find $\bar{\lambda}' \approx \text{const}$ for the full halo sample and $\bar{\lambda}'$ decreasing for the accretion dominated halos in agreement with VK01.

effect, acting similarly on either λ and λ' . Minor mergers continuously bring in a net amount of angular momentum. Large scale gravitational torques therefore seem to dominate the origin of angular momentum in galaxies in conflict with previous ideas that continuous infall occurs from random directions, leading to a zero net effect on $\lambda^{(i)}$.

8 SUMMARY AND DISCUSSION

We performed simulations of large scale structure formation in a Λ CDM universe and extracted all *Friends-of-Friends* selected dark matter halos at 20 distinct redshifts between $z = 2.8$ and $z = 0$. Our principal goal was to investigate the differences of the two commonly used versions of the spin parameter, to understand their behaviour under the influence of halo major mergers and accretion and to determine whether the spin parameter evolution is driven by minor or major mergers.

The spin transfer $T'_\lambda = \lambda_{\text{fin}}^{(i)}/\lambda_{\text{init}}^{(i)}$ for any minor (mM) and major merger (MM) event throughout the simulations was calculated. We find that (1) the probability distribution T'_λ agrees well with the one found by Vitvitska et al. (2004) and (2) the corresponding “classical” quantity T_λ is distributed almost identically. This holds for either minor and major mergers regardless of the considerable distinct values of λ and λ' especially during merger events.

We analysed the spin transfer dependence of the orbital parameters. The pericenter distance between a halo and an infalling satellite was identified as the free parameter which is mainly responsible for the spin transfer T'_λ . This is a result of the high values of $L_{\text{orb}}/J_{\text{int}} > 3(5.7, 11)$ in 80% (50%, 20%) of all major mergers (L_{orb} and J_{int} being the orbital and internal angular momentum, respectively). It is mainly orbital angular momentum that is transferred to internal spin during mergers. The relative orientations between halo and satellite spin vectors turned out to have a minor (but

detectable) influence on $T_{\lambda}^{(l)}$, resulting from similar order-of-magnitude values of internal and orbital angular momentum in a considerable amount of merger events.

In order to further analyse the effect of merger events on the evolution of the spin parameters, we plotted the evolution of $\lambda^{(l)}$ along a fictitious time axis which describes the time relative to the final MM event of each individual halo. It turned out that after the merger onset, $\lambda^{(l)}$ experiences a peaked rise of $\approx 30\%$, and a considerable decline later on. The first is due to relaxation effects, combined with the transformation of orbital to internal angular momentum, while the latter seems to be the result of subsequent mass accretion in combination with a constant mean value of the added specific angular momentum.

The time evolution of the virial coefficient $\eta = 2E_{\text{kin}}/|E_{\text{pot}}|$ and its correlation with the spin parameters was investigated. $\lambda^{(l)}$ is very sensitive to η following $\lambda^{(l)} \approx \alpha + \beta\eta^4$. The values of α and β depend on redshift and the type of the spin parameter. The correlation is stronger for lower redshifts and for the dashed spin parameter λ' . On the fictitious time axis t^* , η shows the same peak-like feature around $t^* = 0$ as the spin parameters, though less pronounced. A strong correlation was found between the ratio λ'/λ and η . While one might not be surprised about a $\lambda^{(l)} - \eta$ correlation in principal (due to the direct or indirect use of the mechanical energies) the detailed origin of this particular behaviour is still an open issue.

We finally examined the redshift evolution of the spin parameters. While the global mean value $\bar{\lambda}'$ turns out to be roughly redshift independent, we find that $\bar{\lambda}$ is significantly increasing with time. If we restrict the halo sample to those which never had major mergers, the picture changes slightly: While λ' is still significantly growing with time, we find λ to decrease moderately. The earlier result of similar $T_{\lambda}^{(l)}$ distributions is not contradicting this result: In fact λ and λ' have mean spin transfers which are different by a small but important amount for the mM sample of halos ($\bar{T}_{\lambda}^{(l)} = 1.007(0.997)$). This causes a significant difference in the global evolution since the "operation" $\lambda^{(l)} \rightarrow T_{\lambda}^{(l)} \times \lambda^{(l)}$ is acting about 18 times on each halo between $z = 2.8$ and $z = 0$. The distinct behaviour of both spin parameters is thus induced by their distinct reactions on minor merger and accretion events. Due to their comparable rare appearance major mergers must be considered as only minor additional corrections to the λ evolution which is dominated by a coordinated action of minor mergers caused probably by large scale stream flows that could be the result of tidal torques.

We like to thank Hans-Walter Rix for enriching comments and general support. This work was supported by the *Deutsche Forschungsgemeinschaft* via *SFB 439, Galaxien im jungen Universum*.

REFERENCES

Barnes, J. & Efstathiou, G. 1987, ApJ, 319, 575
 Barnes, J. & Hut, P. 1986, Nature, 324, 446
 Blumenthal, G. R., Faber, S. M., Flores, R., & Primack, J. R. 1986, ApJ, 301, 27
 Bryan, G. & Norman, M. 1998, ApJ, 495, 80

Bullock, J. S., Dekel, A., Kolatt, T. S., Kravtsov, A. V., Klypin, A. A., Porciani, C., & Primack, J. R. 2001, ApJ, 555, 240
 Burkert, A. & Naab, T. 2003, in Galaxies and Chaos, eds G. Contopoulos & N. Voglis (Springer), p. 327
 Burkert, A. & Naab, T. 2004, in Coevolution of Black Holes and Galaxies, Carnegie Observatories Centennial Symposia, eds L. Ho (Cambridge), p. 422
 Cole, S., A. & Lacey, S., 1996, A&A, 281, 716
 Cole S., Lacey C. G., Baugh C. M., Frenk C. S., 2000, MNRAS, 319, 168
 D'Onghia, E., & Burkert, A. 2004, ApJL, 612, L13
 Ebisuzaki, T., Fukushige, T., Funato, Y., Makino, J., Taiji, M., Hachisu, I. & Sugimoto, D. 1993, Bulletin of the American Astronomical Society, 25, 813
 Fall, S. M., & Efstathiou, G., 1980, MNRAS, 193, 189
 Gardner, J. P. 2001, ApJ, 557, 616
 Götz, M., Huchra, M.P. & Brandenberger, R.H. 2003, preprint (astro-ph/9811393)
 Burkert, A. & d'Onghia, E. 2004, preprint (astro-ph/0409540)
 Hoyle, F. in *Problems of Cosmological Aerodynamics*, 1948, ed. Burgers, J. M. and van der Hulst, H. C. Central Air Documents Office, Dayton OH
 Kauffmann G., White S. D. M., Guiderdoni B., 1993, MNRAS, 264, 201
 Kauffmann, G., Colberg, J. M. Diaferio, A. & White, S.D.M. 1999, MNRAS, 303, 188
 Khochfar, S. & Burkert, A. 2003, preprint (astro-ph/0309611)
 Ma, C. & Bertschinger, E. 1995, ApJ, 455, 7
 Makino, J. & Funato, Y. 1993, PASJ, 45, 279
 Maller, A. H., Dekel, A., & Somerville, R. 2002, MNRAS, 329, 423
 Mo H. J., Mao S., White S. D. M., 1998, MNRAS, 295, 319
 Naab, T., Burkert, A., & Hernquist, L. 1999, ApJL, 523, L133
 Navarro, J.F., Frenk, C.S. & White, S.D.M. 1996, ApJ, 462, 563
 Navarro, J.F., & Steinmetz, M. 2000, ApJ, 538, 477
 Padmanabhan, T. 1993, Cambridge, UK: Cambridge University Press, —c1993,
 Pearce, F. R. & Couchman, H. M. P. 1997, MNRAS, 2, 411
 Peebles, P. J. E. 1980, Research supported by the National Science Foundation. Princeton, N.J., Princeton University Press, 1980. 435 p.,
 Peirani, S., Mohayaee, R., & de Freitas Pacheco, J. A. 2004, MNRAS, 348, 921
 Primack, J. R. 2004, IAU Symposium, 220, 467
 Shapiro, P.A., Iliev, I.T., Martel, H., Ahn, K. and Alvarez, A., 2004, preprint (astro-ph/0409173)
 Somerville R. S., Primack J. R., Faber S. M., 2001, MNRAS, 320, 504 ! MNRAS FORMAT
 Spergel, D. N., et al. 2003, ApJ Supp, 148, 175
 Toomre, A. & Toomre, J. 1972, ApJ, 178, 623
 van den Bosch F. C., 2000, ApJ, 530, 177
 Vitvitska, M., Klypin, A. A., Kravtsov, A. V., Wechsler, R. H., Primack, J. R., & Bullock, J. S. 2002, ApJ, 581, 799
 White S. D. M., Efstathiou G., Frenk C. S., 1993, MNRAS, 262, 1023
 White, S.D.M., & Rees, M.J., 1978, MNRAS, 183, 341